

NOAA Technical Memorandum ERL PMEL-72

MEASUREMENTS OF BENTHIC SEDIMENT ERODIBILITY IN PUGET SOUND, WASHINGTON

J. W. Lavelle

W. R. Davis
EPA/Environmental Research Laboratory
South Ferry Road
Narragansett, Rhode Island

Pacific Marine Environmental Laboratory
Seattle, Washington
May 1987



**UNITED STATES
DEPARTMENT OF COMMERCE**

**Malcolm Baldrige,
Secretary**

**NATIONAL OCEANIC AND
ATMOSPHERIC ADMINISTRATION**

**Anthony J. Calio,
Administrator**

**Environmental Research
Laboratories**

**Vernon E. Derr,
Director**

NOTICE

Mention of a commercial company or product does not constitute an endorsement by NOAA/ERL. Use of information from this publication concerning proprietary products or the tests of such products for publicity or advertising purposes is not authorized.

For sale by the National Technical Information Service, 5285 Port Royal Road
Springfield, VA 22161

Contribution No. 919 from NOAA/Pacific Marine Environmental Laboratory

CONTENTS

	<u>PAGE</u>
ABSTRACT.....	1
1. INTRODUCTION.....	1
2. BACKGROUND.....	4
3. METHODS.....	7
4. RESULTS AND DISCUSSION.....	16
5. CONCLUSIONS.....	27
6. ACKNOWLEDGMENTS.....	29
7. REFERENCES.....	30

MEASUREMENTS OF BENTHIC SEDIMENT ERODIBILITY IN PUGET SOUND, WASHINGTON

J.W. Lavelle¹
W.R. Davis²

ABSTRACT. Rates of erosion of bottom sediment were studied at seven locations in Puget Sound, Washington. Fresh, unremoulded sediment from box cores was exposed to turbulence in a fluid chamber in which turbulence is generated by oscillating a perforated disk at controlled frequencies. Resulting time series of particulate concentration in the chamber at each stepped level of equivalent bottom stress were used to calculate estimates of erosion rates and deposition velocities. Resulting rates of erosion at 1 dyne/cm² do not appear to be consonant with rates at higher stress, suggesting that a thin surficial layer of sediment is more easily eroded than sediment below. Differences of erosion rates among sites at stresses of 2 dynes/cm² and above are not resolvable with the available data.

1. INTRODUCTION

Calculating the movement of marine sediment is often possible if the erosional response of the sediment to stress imposed by the overlying flow is known. In most estuaries, however, calculations are made difficult because there is little information available about entrainment rates of sediment. This is true of Puget Sound where only one rate estimate is available, though rates might well be expected to vary considerably in place and time. This report describes an attempt to begin to identify the variability of entrainment rates within the Sound using an easily employed technique.

Rates of erosion depend on sediment texture, porosity, biological content, and possibly other factors. The expectation of differences in erosion rates in Puget Sound stems from the high variability in sediment texture (Roberts, 1974; Baker, 1984), porosity (Lavelle et al., 1986), and

¹ Pacific Marine Environmental Laboratory, 7600 Sand Point Way N.E., Seattle, WA, 98115-0070

² EPA/Environmental Research Laboratory, South Ferry Road, Narragansett, RI, 02882

infaunal content (Nichols, 1975). The only estimate of erosion rate available for Puget Sound up until this time is based on near-bottom current and optical transmission time series (Lavelle et al., 1984). Measurements of that type depend on natural currents having sufficient strength and range during the time of observation to provide observable and interpretable signals. A second, more difficult approach is to induce stress on the bottom using an *in-situ* flume (e.g. Young, 1977) and observe the resuspension. Such devices have yet to be made quantitative in terms of estimating erosion rates. A third method of obtaining rates, and the procedure used here, involves the introduction of zero-mean-shear turbulence to a sediment surface. The turbulence provides instantaneous stresses with strengths similar to those caused by steady shear flows. A device with this capability was first used by Rouse (1938) and reintroduced for application to fine lacustrine sediment by Tsai and Lick (1986).

The objective of our study was to examine the potential of the Tsai and Lick (1986) resuspension device for estuarine application, to quantify erosion rates of sediment for different sites in Puget Sound, and to compare these estimates with each other and with the earlier estimate based on an entirely different estimation procedure. Because the work was in part a feasibility study, some of the discussion is devoted to the uncertainties of the measurements and to improving future results.

Samples for erosion analysis come from seven box-cores taken in Puget Sound in August, 1986 (Fig. 1, Table 1). Two cores were acquired at the Four-Mile Rock Dump Site in Elliott Bay, a three core transect was taken across the main basin off Shilshole Bay, a single core was taken in the center of the basin off Point Wells, and one core was taken at the southern end of Hood Canal. The central Shilshole Bay and Point Wells cores were taken in the

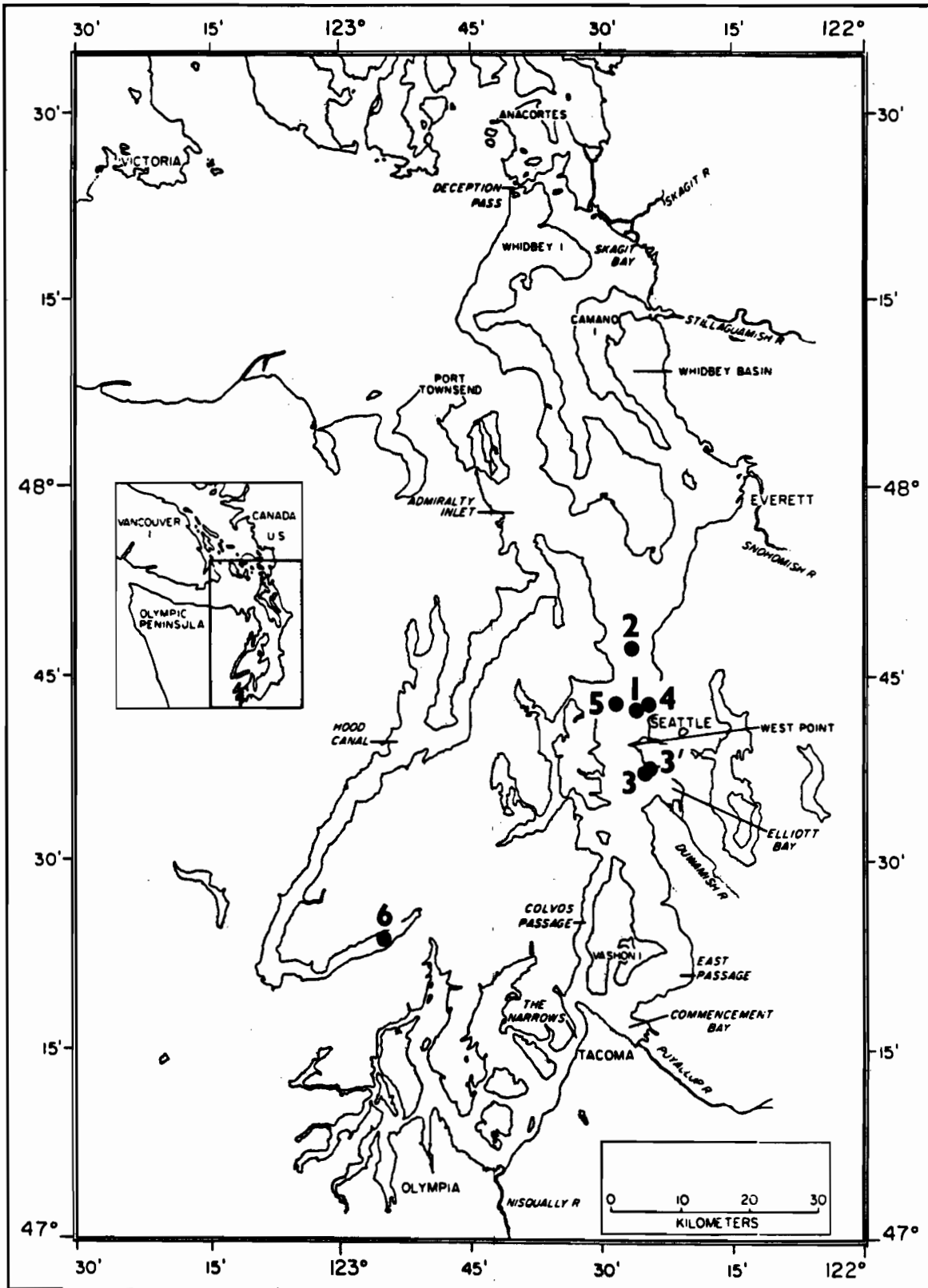


Figure 1.--Location map of coring sites.

Table 1.--Location of box cores.

Core #	Locator Name	Latitude	Longitude	Depth (m)
1	Shilshole-Central	47°42.01'	122°26.10'	206
2	Point Wells	47°46.80'	122°26.49'	193
3	Four Mile Rock	47°37.12'	122°25.00'	175
3'	Four Mile Rock	47°37.43'	122°24.54'	133
4	Shilshole-East	47°42.49'	122°24.69'	105
5	Shilshole-West	47°42.50'	122°28.30'	179
6	Hood Canal	47°24.30'	122°54.90'	16

proximity of moorings that were recording current speed and optical transmission at points 1, 4, and 15 m from the seafloor. The central Shilshole Bay site was also near the location of previous boundary layer studies (Lavelle et al., 1984).

2. BACKGROUND

A device for generating zero-mean-shear turbulence using vertically oscillated grids was first employed by Rouse (1938) in sediment resuspension experiments. Subsequently Murray (1969) simulated wave resuspension using oscillating grids. Tsai and Lick (1986) have recently developed an oscillating disk device (Fig. 2) for investigating Great Lakes sediment resuspension. Davis and MacIntyre (in press) used the same device in Long Island Sound for studying biological factors influencing entrainment.

Oscillating grid turbulence devices have seen considerable use in problems of entrainment of fluids across density interfaces (e.g. Rouse and Dodu, 1955; Cromwell, 1960; Turner and Kraus, 1967). These entrainment

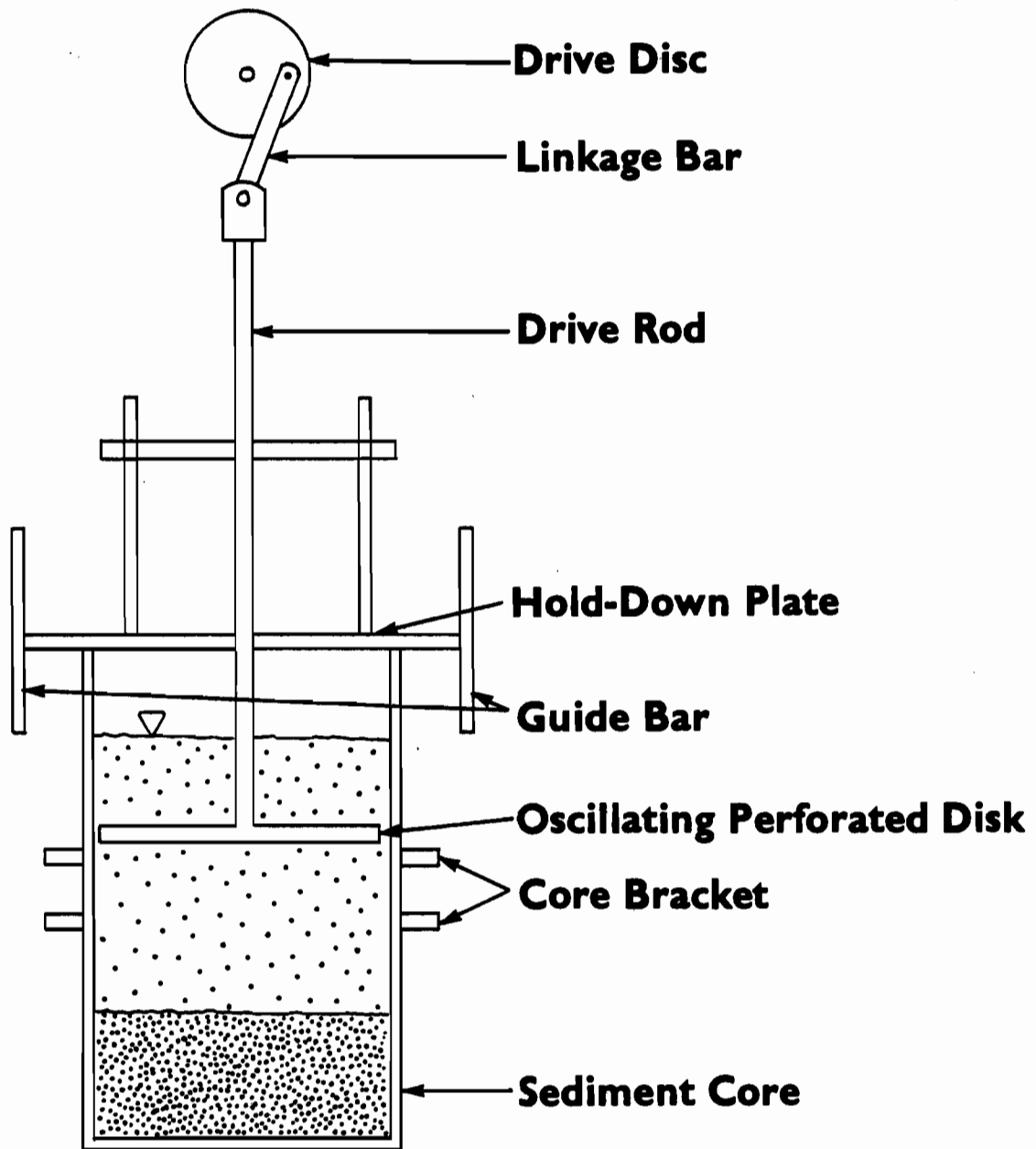


Figure 2.--Schematic diagram of the device used to entrain sediments (Tsai and Lick, 1986).

studies have lead to detailed measurements of the turbulence structure within oscillating grid chambers (e.g. Bouvard and Dumas, 1967; Thompson and Turner, 1975; Hopfinger and Toly, 1976; McDougall, 1979; E and Hopfinger, 1986) and to theoretical descriptions (Long, 1978). Dependencies of turbulence on the oscillation frequency, distance from the grid, stroke length, and mesh size and form have all been probed. While it is clear that the turbulence field generated by such a device is different than that generated by a shear flow, corresponding conditions can be found for which entrainment rates, that depend on instantaneous turbulence stresses in the boundary layer in both types of flow, can be made identical.

The conceptual picture of sediment resuspension by Grass (1983) proves useful in understanding the resuspension by the oscillating disk device used in these experiments. Grass (1983) reviews observations on ejections and intrushes of turbulent fluid through the near-bed region and on single particle resuspension. He documents that both near-bed instantaneous stress (e.g. $-u'w'$, where u' and w' are horizontal and vertical velocity fluctuations), which characterizes the strength of the intrush/ejection event, and individual particle threshold stress (not bed threshold stresses, see Lavelle and Mofjeld (1987)) are distributed properties. Thus, even though the mean turbulent stress may be much smaller than the mean particle threshold stress, erosion of the bed can still occur intermittently. If the two distributions overlap, some instantaneous stress values will occasionally exceed some particle threshold stress values. The larger the distributional overlap, the greater the likelihood of instantaneous particle resuspension. Instantaneous stresses, not mean stress, determine the occurrence of resuspension both in the oscillating disk device and in steady shear flow. For the special case of steady shear flow, however, a relationship between the statistics of the

instantaneous stress distribution might be expected, e.g. between the mean bottom-stress value and the probability of instantaneous stresses sufficiently large to cause resuspension. Consequently, for steady shear flow, it is conventional to relate erosion/resuspension to mean bottom-stress levels.

Because resuspension in steady turbulent flow is usually related to mean rather than instantaneous stress, it is convenient to relate the results from the oscillating disk device to equivalent condition in steady flow. By equivalent conditions we mean steady-flow stress levels that lead to the same rate of entrainment. For zero-mean and non-zero-mean stress devices in which turbulence intensity is sufficiently large to create a vertical uniform concentration of resuspended material, the condition of equivalency occurs when concentrations in both devices are identical (see below). Consequently, oscillation frequencies for the Tsai and Lick (1986) device have been related to equivalent steady-flow mean stress by comparison of concentrations to those measured in a shallow annular flume. Our results are reported in terms of those equivalent near bottom stresses rather than in terms of oscillation frequencies.

3. METHODS

At each station (Fig. 1), sediment was acquired by standard box core with surface dimensions of 21 cm by 30.5 cm. Flaps on the corer near the top of the box closed as the core was pulled out of the bottom, limiting the disturbance of the surficial sediment as the core was drawn to the sea surface. On deck, two subsamples (plugs) from each core were carefully taken by partially inserting lengths of 12.7 cm (5 in) diameter acrylic pipe into the core. Locations of these plugs of sediment within each box were chosen to avoid box edges, to capture material representative of the surface, and to

avoid any visible disturbance resulting from the coring. Bottom caps were slid under the tubes now partially filled with sediment. The volume overlying the sediment was then filled with seawater and each plug set aside while slowly flowing seawater refreshed the overlying fluid. Flow rates were restricted to prevent suspension and loss of the uppermost layer of sediment.

Subsequently, each sample in turn was securely positioned in the resuspension device (Fig. 2). The apparatus consists of a variable speed motor connected to a perforated flat plate that is oscillated at selectable frequencies in the fluid overlying the sediment. Details on the configuration of the device are to be found in the paper of Tsai and Lick (1986). At each frequency, subsamples of the supernatant are drawn over time through a side port in the chamber (acrylic tube) walls. At each frequency, sampling continues until equilibrium concentration is reached, and then the oscillation frequency is increased.

The oscillation frequency has been empirically correlated with bottom stress (Fig. 3) in experiments conducted by Tsai and Lick (1986). This was done by matching suspended sediment concentrations in the resuspension device at various oscillation frequencies (0.08-0.14/s) with those in an annular flume for which the bottom stress ($\sim 2-4$ dynes/cm²) had been measured by the velocity profile method. Identical sediments and bed-preparation procedures were used in both devices. The water level, mean disk position from the bed, and stroke length in the oscillating disk device in those and in our experiments were fixed at 12.7 cm (5 in), 6.3 cm (2.5 in), and 2.5 cm (1 in) respectively. Oscillation frequencies for stress levels of 1 dyne/cm² are based on extrapolation of those measurements and are subject to future verification.

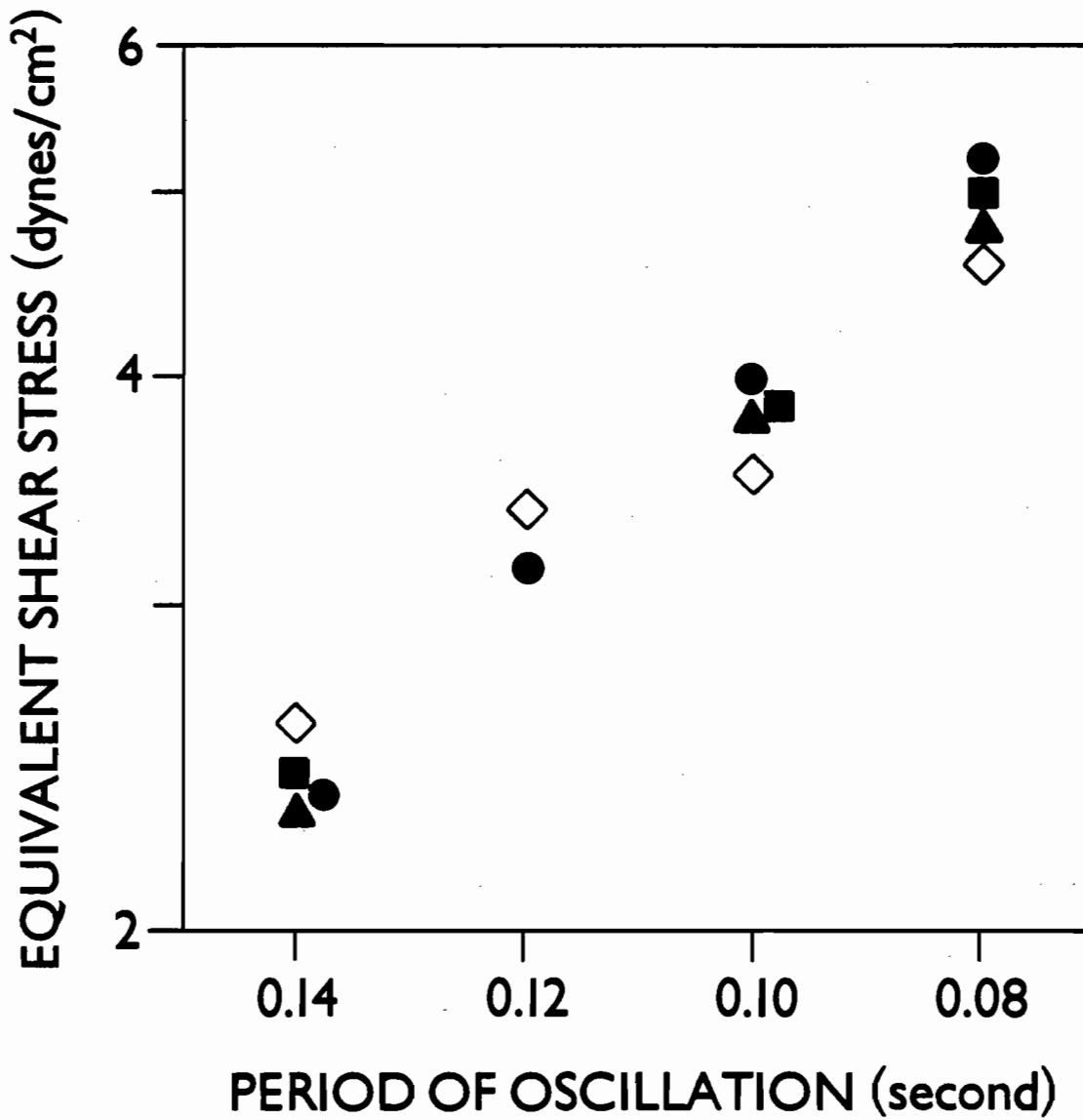


Figure 3.--Empirical relationship between disk oscillation frequency and equivalent bottom stress from Tsai and Lick (1986). Closed and open symbols represent two and seven days consolidation of sediment prior to experiments.

Each of the core samples was exposed to equivalent bottom stresses of 1, 2, 3, 4, and 5 dynes/cm². At each level of stress, net erosion occurred over time until an equilibrium concentration, as judged by turbidity, was reached (Fig. 4). In some cases this took approximately 100 minutes to achieve even though the fluid volume in the chamber (1.6 l) was small. At each level of stress, numerous small subsamples were drawn out of the resuspension device and their turbidity measured. Those subsamples were returned to the chamber after turbidity measurements to conserve volume and suspended solids.

Turbidity of the subsamples was measured at a wavelength of 660 nm with a Bausch and Lomb Spec 20 spectrophotometer. At equilibrium turbidity for each equivalent stress level, samples were also filtered and weighed. The mass concentration versus light attenuation data as a composite from all cores are shown in Fig. 5. At high concentrations the data show the effects of multiple scattering of light off sediment particles interposed in the light path (e.g. Ward and Chikwanha, 1980). Nearly complete quenching of light transmission occurs at concentrations of 3000 mg/l and beyond.

For fixed distributions of particle size, index of refraction, and light path length, the dependence of fractional light transmission, T, on concentration can be given the empirical form (Ward and Chikwanha, 1980):

$$T = e^{-\gamma \left(\frac{C}{C_R}\right)^\beta} \quad (1)$$

Here $T = I/I_0$, where I is the transmitted and I_0 the incident light intensity, C is the particulate mass concentration, γ is an attenuation coefficient, C_R is a reference concentration, and the exponent β accounts for the effects of multiple scattering at high concentrations. For the small path length in the photospectrometer ($l = 1.0$ cm) and the large concentrations studied, no clear water attenuation effects need be considered.

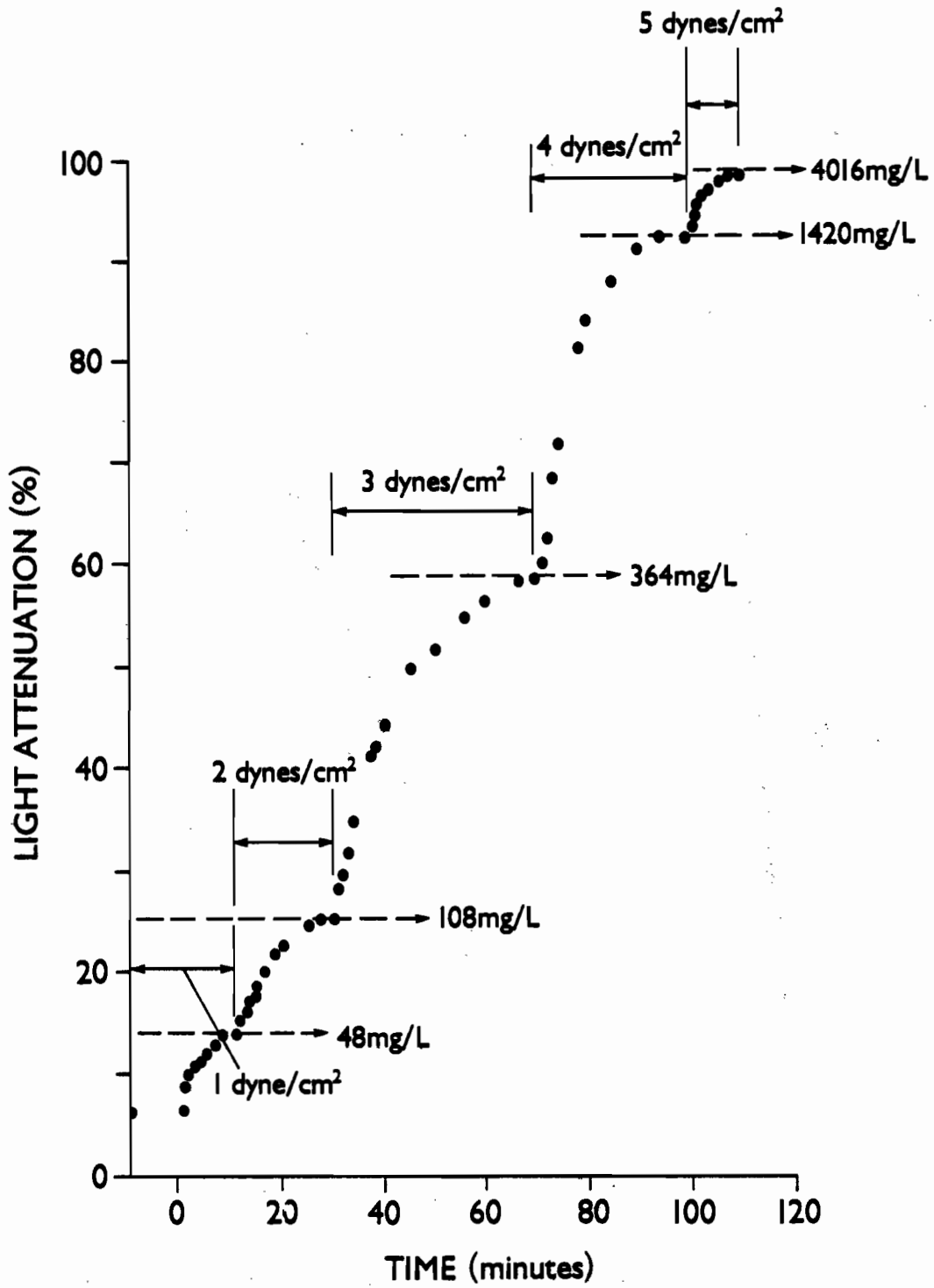


Figure 4.--Time series of light attenuation in subsamples drawn from the entrainment chamber over intervals of constant equivalent bottom stress. Data comes from the Shilshole-central core.

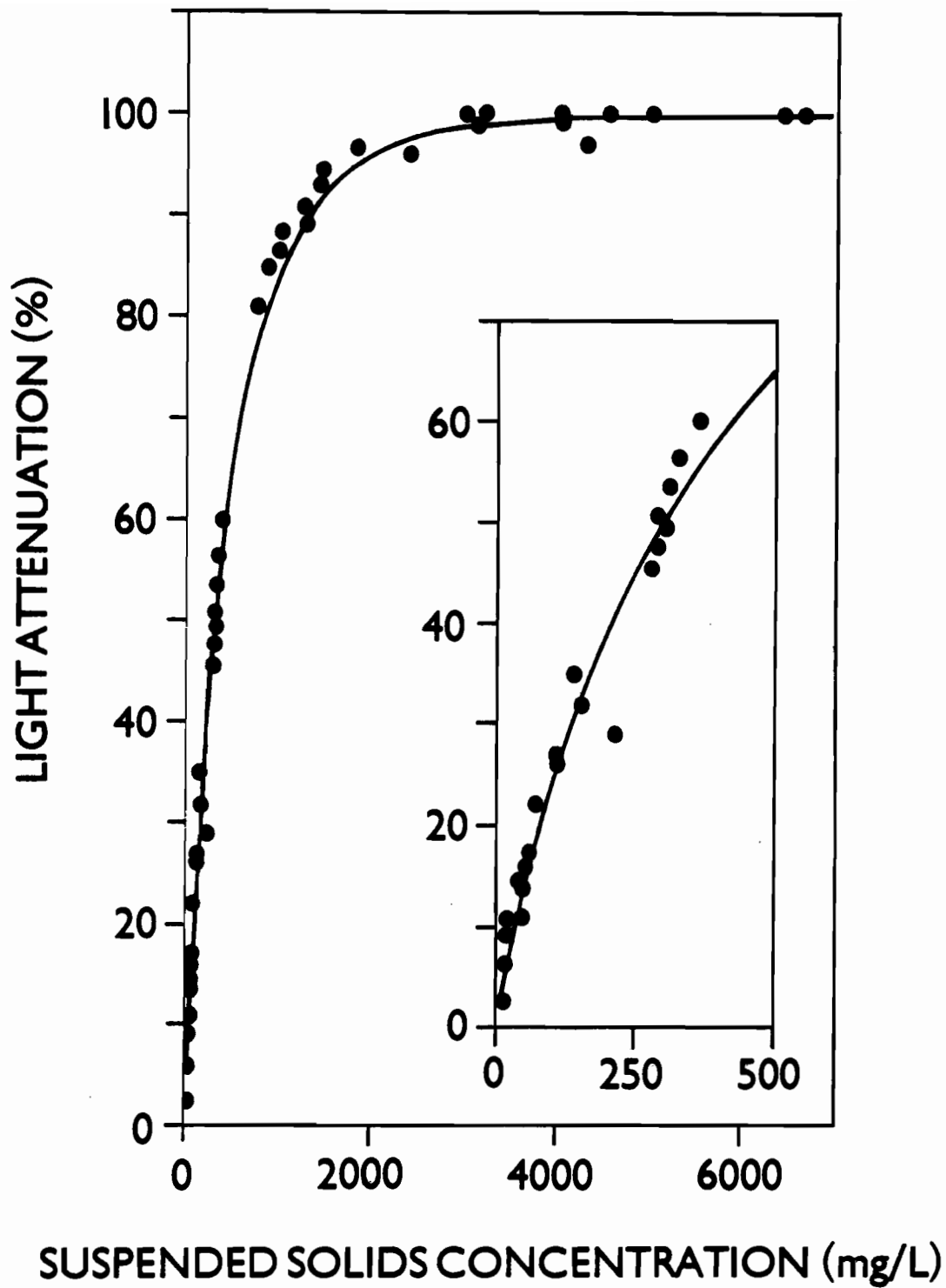


Figure 5.--Light attenuation and mass concentration data (dots) and the inferred calibration curve (line). Data is a composite for all cores.

The data of Fig. 5 were least-squares fitted for γ and β with the linear equation:

$$\ln (-\ln T) = \ln (\gamma) + (\beta) \ln (C/C_R) \quad (2)$$

where C_R is given a value of 500 mg/l, and T is the complement with respect to one of percent light attenuation divided by 100. The fit gives a value for β of 0.8, and a value of γ of 1.05. The best fit curve (Fig. 5) was used to reexpress all attenuation measurements as mass concentrations.

Mass concentration time series at fixed stress (e.g. in Fig. 4) can be used to calculate erosion rates under these conditions in the mixing chamber: 1) there is no radial dependence to erosion or concentration; 2) there is little vertical dependence to the concentration at the imposed stresses; 3) the resuspended material can be considered to have a single deposition velocity. Then it is reasonable to expect mass conservation in one-dimensional form:

$$\frac{\partial C}{\partial t} + \frac{\partial}{\partial z} (w_s C) - \frac{\partial}{\partial z} \left[A_z \frac{\partial C}{\partial z} \right] = 0 \quad (3)$$

where C is the mass concentration, t is time, z is the vertical coordinate (positive upward), w_s is particle settling velocity, and A_z is the vertical eddy diffusivity. The flux at the upper surface of the container must be zero:

$$w_s C - A_z \frac{\partial C}{\partial z} = 0, \quad z = h \quad (4)$$

where h is the height of the fluid column (12.7 cm). At the sediment-water interface; the upward flux is equal to a sum of two terms (e.g. Parthenaides, 1972):

$$w_s C - A_z \frac{\partial C}{\partial z} = E - w_d C, \quad z = 0 \quad (5)$$

where E is the erosion rate and w_d is the deposition velocity.

If Eq. 3 is integrated over the depth of the fluid and the boundary conditions imposed, the depth-averaged (and presumably measured) concentration, \bar{C} , has this time dependence:

$$\frac{\partial}{\partial t}(\bar{C}h) = E - w_d C(0) \quad (6)$$

If \bar{C} and $C(0)$ are considered equal by virtue of the near vertical homogeneity of concentration, $C(0)$ may be replaced with C and Eq. 6 integrated in time to give:

$$\bar{C} = C_0 e^{-(w_d/h)t} + \frac{E}{w_d} [1 - e^{-(w_d/h)t}] \quad (7)$$

C_0 is the depth averaged concentration at the start of that stress stage. Note that the vertical turbulence structure plays no explicit role in this equation, though the assumptions of near vertical uniformity of concentration requires vigorous mixing. Direct confirmation by measurement of the radial and vertical distributions of concentration have yet to be made, though the vigorous mixing observed occurring in the apparatus at stresses of 1 dyne/cm² or greater make it likely.

Eq. 7 can be used to show that at the start of each stage, $t = 0$:

$$\begin{aligned}\alpha_1 &\equiv \left. \frac{\partial \bar{C}}{\partial t} \right|_{(t=0)} \\ &= \frac{E}{h} - \frac{w_d}{h} C_0\end{aligned}\quad (8)$$

and at equilibrium ($t \rightarrow \text{large}$):

$$\alpha_2 \equiv \bar{C}(t \rightarrow \infty) = \frac{E}{w_d} \quad (9)$$

Both α_1 and α_2 can be estimated from the data. Knowing α_1 , α_2 , and C_0 allows both E and w_d to be calculated:

$$E = \frac{\alpha_1 h}{(1 - C_0/\alpha_2)} \quad (10)$$

$$w_d = \frac{\alpha_1 h}{\alpha_2 (1 - C_0/\alpha_2)} \quad (11)$$

The entrainment rate depends on the initial concentration, its time rate of change, and the equilibrium concentration, but it is not explicitly dependent on eddy diffusivity or turbulence intensity in this case.

Erosion rates and deposition velocities were calculated from the time series data using Eqs. 10 and 11. Values for α_1 ($-\Delta C/\Delta t$) were evaluated for data pairs for which the elapsed time, Δt , was less than or equal to 5 minutes. Few cores had data as temporally dense as shown in Fig. 4, and therefore erosion rates for some cores at some stress levels could not be evaluated. Another approach to evaluating E and w_d would be to least-squares

fit Eq. 7 directly to each constant stress segment of data (Fig. 4) with E and w_d as parameters.

Particle size distribution of selected samples were also measured aboard ship using a Coulter Counter. Standard Coulter Counter techniques (e.g. Kranck and Milligan, 1979) were used.

4. RESULTS AND DISCUSSION

A qualitative description of the core from each station is found in Table 2. There were considerable differences among the cores both in apparent sediment texture and infaunal species and abundances. The Four Mile Rock Core #3 was silt and clay while containing many large and small pieces of decaying wood, but the Four Mile Rock Core #3' was primarily coarse sand and gravel. The Shilshole-East core had pebbles on a surface of soft mud and pebbles throughout its depth; how pebbles at the surface would not have been covered by depositing muds is difficult to explain. The Hood Canal core was the most intensely bioturbated and because of little apparent clay content was easily eroded.

Results of the quantitative analysis for erosion rate, E , and deposition velocity, w_d , for each core is given in Table 3. The elapsed time, Δt , used in calculating α_1 (Eq. 8) is explicitly given. For a few cases, a high density of samples in the first few minutes after stress was imposed permit a comparison of erosion rates when Δt takes different values. Rates tend to show a systematic decline as Δt increases, even over the first several minutes (Table 3). Consequently, stress levels for which changes in concentration were not measured within 5 minutes of stress initiation are of dubious value and have not been tabulated.

Table 2.--Core qualities from visual inspection.

Box Core #	Locator Name	Qualities
1	Shilshole-Central	Silt-clay, minor sand content bioturbated (Pectinaria) non-plastic watery surface
2	Point Wells	Silt-clay, minor sand content bioturbated non-plastic surface copepods in overlying water or sediment surface
3	Four Mile Rock	Silt-clay, minor sand content large and small pieces of rotting wood black veins in brown muds bioturbated very soft, non-plastic surface ("fluffy"), possible core surface distortion
3'	Four Mile Rock	coarse sand-gravel-rock with clay deposits clay strata/deposits only cohesive structure no macrofauna (2 mm sieve)
4	Shilshole-East	Silt-clay infiltrated with sand-gravel (CA. 50%) gravel on surface 0.75" surface relief
5	Shilshole-West	Silt-Clay, minor sand content bioturbated, larger fewer forms 0.75--1.5" surface relief worm tubes, core surface distortion
6	Hood Canal	Mostly silt, little clay apparent (no stickiness), most intense bioturbation

Table 3.--Erosion rates and deposition velocities at each value of stress.

Core # -Plug #	Locator Name	Stress* (dynes/cm ²)	Δt (min)	E (g/cm ² /s)	w _d (cm/s)
1-1	Shilshole-Central	1	0.5	5.3 × 10 ⁻⁶	1.2 × 10 ⁻¹
"	"	1	1.0	3.7 × 10 ⁻⁶	8.7 × 10 ⁻²
"	"	1	2.0	2.6 × 10 ⁻⁶	6.1 × 10 ⁻²
"	"	1	3.0	2.0 × 10 ⁻⁶	4.6 × 10 ⁻²
"	"	2	0.5	3.4 × 10 ⁻⁶	3.2 × 10 ⁻²
"	"	2	1.0	3.1 × 10 ⁻⁶	3.0 × 10 ⁻²
"	"	2	2.0	2.3 × 10 ⁻⁶	2.2 × 10 ⁻²
"	"	2	3.0	1.9 × 10 ⁻⁶	1.8 × 10 ⁻²
"	"	3	0.5	5.1 × 10 ⁻⁶	1.3 × 10 ⁻²
"	"	3	1.0	5.9 × 10 ⁻⁶	1.4 × 10 ⁻²
"	"	3	2.0	5.4 × 10 ⁻⁶	1.4 × 10 ⁻²
"	"	3	3.5	4.5 × 10 ⁻⁶	1.1 × 10 ⁻²
"	"	4	0.5	7.4 × 10 ⁻⁶	4.6 × 10 ⁻³
"	"	4	2.0	8.3 × 10 ⁻⁶	5.2 × 10 ⁻³
"	"	4	3.0	1.5 × 10 ⁻⁵	9.3 × 10 ⁻³
"	"	5	0.5	8.4 × 10 ⁻⁵	2.4 × 10 ⁻²
"	"	5	1.0	1.0 × 10 ⁻⁴	3.0 × 10 ⁻²
"	"	5	2.0	9.3 × 10 ⁻⁵	2.7 × 10 ⁻²
1-2	Shilshole-Central	2	2.0	1.4 × 10 ⁻⁶	1.7 × 10 ⁻²
"	"	3	3.0	4.7 × 10 ⁻⁶	1.3 × 10 ⁻²
"	"	4	5.0	1.6 × 10 ⁻⁵	1.4 × 10 ⁻²
"	"	5	5.0	4.4 × 10 ⁻⁵	8.4 × 10 ⁻³
2-1	Point Wells	3	2.0	2.4 × 10 ⁻⁵	2.1 × 10 ⁻²
"	"	4	2.0	3.8 × 10 ⁻⁵	1.7 × 10 ⁻²
2-2	Point Wells	3	2.0	8.1 × 10 ⁻⁶	3.0 × 10 ⁻²
"	"	4	2.0	2.7 × 10 ⁻⁵	1.9 × 10 ⁻²
3-1	Four Mile Rock	1	2.0	6.7 × 10 ⁻⁶	4.1 × 10 ⁻²
"	"	2	2.0	2.5 × 10 ⁻⁶	8.3 × 10 ⁻³
"	"	3	2.0	1.2 × 10 ⁻⁵	1.4 × 10 ⁻²
"	"	4	3.0	5.3 × 10 ⁻⁵	2.6 × 10 ⁻²
3-2	Four Mile Rock	1	2.0	7.4 × 10 ⁻⁶	5.2 × 10 ⁻²
"	"	2	2.0	7.7 × 10 ⁻⁶	2.6 × 10 ⁻²
"	"	3	2.0	2.5 × 10 ⁻⁵	2.5 × 10 ⁻²
"	"	4	2.0	1.4 × 10 ⁻⁵	8.1 × 10 ⁻³
"	"	5	2.0	6.7 × 10 ⁻⁵	1.3 × 10 ⁻²
3 ¹ -1	Four Mile Rock	4	2.0	5.7 × 10 ⁻⁶	3.0 × 10 ⁻²
"	"	5	2.0	4.7 × 10 ⁻⁶	1.5 × 10 ⁻²
4-1	Shilshole-East	2	2.0	2.3 × 10 ⁻⁷	9.3 × 10 ⁻³
"	"	3	2.0	1.9 × 10 ⁻⁶	3.6 × 10 ⁻²
"	"	4	2.0	2.4 × 10 ⁻⁶	2.1 × 10 ⁻²
"	"	5	3.0	4.8 × 10 ⁻⁶	1.4 × 10 ⁻²
4-2	Shilshole-East	2	1.0	4.2 × 10 ⁻⁷	8.4 × 10 ⁻²
"	"	3	0.5	3.7 × 10 ⁻⁶	2.5 × 10 ⁻¹
"	"	3	1.0	4.7 × 10 ⁻⁷	3.1 × 10 ⁻²
"	"	3	2.0	5.8 × 10 ⁻⁷	3.8 × 10 ⁻²
"	"	4	2.0	1.0 × 10 ⁻⁶	2.4 × 10 ⁻²
"	"	5	4.0	3.6 × 10 ⁻⁶	1.4 × 10 ⁻²
5-1	Shilshole-West	3	2.0	4.3 × 10 ⁻⁵	3.1 × 10 ⁻²
5-2	Shilshole-West	3	2.0	3.1 × 10 ⁻⁵	4.2 × 10 ⁻²
6-1	Hood Canal	1	3.0	2.2 × 10 ⁻⁶	1.8 × 10 ⁻²
"	"	2	0.5	3.4 × 10 ⁻⁵	1.7 × 10 ⁻²
"	"	2	3.0	1.9 × 10 ⁻⁵	1.0 × 10 ⁻²
"	"	3	3.0	2.2 × 10 ⁻⁵	4.8 × 10 ⁻²

*Stress values of 1 dyne/cm² are based on extrapolation (Fig. 3).

Rates of erosion span the range 4.2×10^{-7} to 1.0×10^{-4} g/cm²/s. This large range in part reflects the non-linear dependence of erosion rate on bottom stress. At a common level of stress (3 dynes/cm²), rates among sites vary by a factor of 20 (Fig. 6). The transect across the main basin off Shilshole Bay shows a large range of rate variation, rates being largest at the western site, and smallest at the eastern site where surficial gravel was found. Replicate pairs suggest the uncertainty in rates is as much as a factor of five, however. In addition, the surfaces of the Four Mile Rock (#3) and Shilshole-Central cores were somewhat disturbed in subsampling and the accuracy of the rates may be questioned. On the other hand, the large differences in rates at the two Four Mile Rock stations (at a common stress of 4 dynes/m², not shown) are most certainly the result of the large difference in sediment texture at the two sites.

Erosion rates are plotted against equivalent bottom stress for stations of four or more data points in Fig. 7. Open and solid points represent results of measurements on replicate samples from each core. For stress values between 2 and 5 dynes/cm², these data conform to a power law dependence of erosion rate on stress, a dependence previously noted for laboratory erosion data (Lavelle et al., 1984). The solid lines in Fig. 7 represent the least square fit of the equation $E = \alpha |\tau/\tau_0|^\eta$ to each set of data, where τ is the bottom stress, and τ_0 is a reference stress of 1 dyne/cm². Estimated values and their 95% confidence limits (Chatterjee and Price, 1977) for the parameters α and η are given in Table 4. Values of α range from 7.9×10^{-8} to 6.3×10^{-7} g/cm²/s, while η varies between 2.5 and 3.4. The Point Wells and Four Mile Rock rates are not significantly larger statistically than the Shilshole-Central and East rates over the stress range of 2-5 dynes/cm²; the large confidence intervals on the parameter estimates (Table 4) prevent

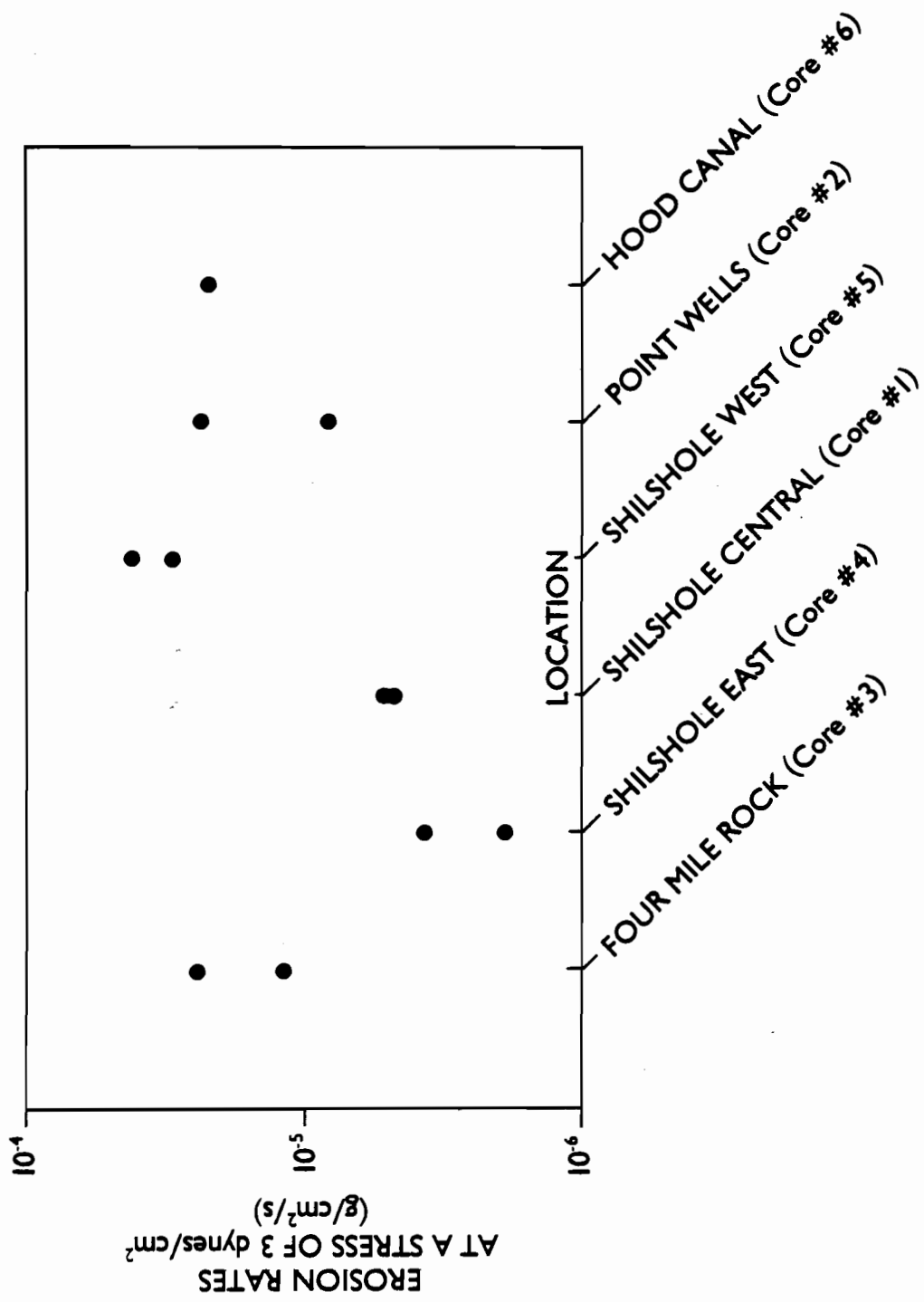


Figure 6.--Comparison of erosion rates at an equivalent stress of 3 dynes/cm² for all stations.

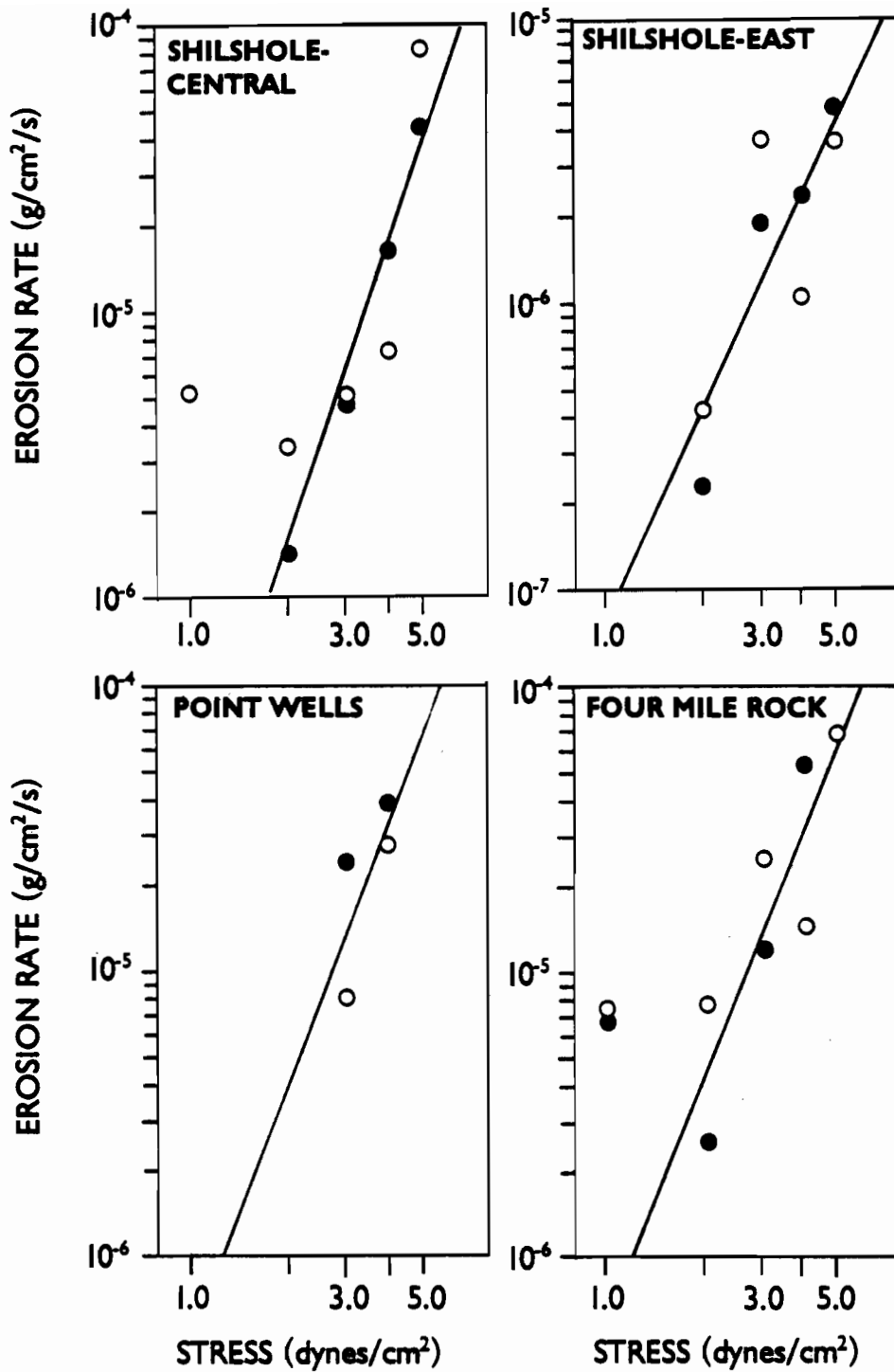


Figure 7.--Rates of erosion versus equivalent bottom stress for stations of four or more data points. Data at stresses less than 2 dynes/cm² were not included in the least-squares fit (solid line). Open and solid points differentiate the results of replicate entrainment experiments.

Table 4.--Erosion rate constants and their 95% confidence intervals when
 $E = \alpha |\tau/\tau_0|^\eta$.

Core #	Locator Name	$\log_{10}\alpha^*$	η	degrees of freedom, N-2
1	Shilshole-Central	-6.8±0.8	3.4±1.5	6
2	Point Wells	-6.3±4.6	2.9±8.5	2
3	Four Mile Rock	-6.2±0.9	2.8±1.8	5
4	Shilshole-East	-7.1±0.9	2.5±1.7	6

* Units for α are g/cm²/s.

resolution of differences in erosion rates for these four sites.

Consequently, the significance of the scatter in the erosion rates at the single stress value of 3 dynes/cm² for all sites (Fig. 6) must be held suspect.

The data allow only a few rates at a stress of 1 dyne/cm² to be calculated. A few such points (Fig. 7), however, suggest that these rates are inconsistent with the erosion law least-square fitted to the other data. At 1 dyne/cm², erosion rates are comparable in magnitude to rates at 2-3 dynes/cm². One interpretation is that the top layer of core, and consequently the layer first entrained, is more easily eroded than sediment deeper in the core. Thus rates calculated at a stress of 1 dyne/cm² represent erosion of a surficial "fluff" layer, while erosion rates discussed up to this point are for more consolidated sediments. A second interpretation is that the oscillating disk itself compresses and artificially consolidates the sediment, a point raised by Tsai and Lick (1986). Experiments run after the initial experiment at 1 dyne/cm² could have been performed on a modified

sediment column. Tsai and Lick (1986) used fresh samples at each stress level to ameliorate this problem. A third possibility is that the rate estimate is in error because of vertical non-uniformity of concentration in the turbulence chamber at stress of 1 dyne/cm². A fourth interpretation is that the extrapolation of oscillation frequency to 1 dyne/cm² is not realistic. The first interpretation seems most probable to us, but the other three cannot be ruled out at this time.

The thickness, ℓ , of the layer resuspended at a stress of 1 dyne/cm² can be estimated:

$$\ell = \frac{C_e h}{\rho_s (1 - \phi)} \quad (12)$$

where C_e is the equilibrium concentration, h is the fluid height in the chamber, ρ_s is the sediment dry-weight density, and ϕ is the porosity of the bed. If ϕ is given a value of 0.95, ρ_s is given a value of 2.6 g/cm³, and the concentration at equilibrium is approximately 150 mg/l, then ℓ is ~0.15 mm. This is comparable to the estimate of the resuspended layer thickness under natural conditions coming from analysis of transmissometer data (Lavelle et al., 1984). Visual observations also suggest a loose layer of sediment at the top of the sediment column. Lavelle et al. (1984) argue that this layer must be composed of particles newly arrived at the sediment-water interface because the high rate of sedimentation in Puget Sound causes particles to be buried below the horizon from which they would normally be resuspended in 5-10 days. That a thin (~0.1 mm) surficial layer of sediment can be resuspended by the oscillating disk device at low stress also suggests the use of the device in sampling the surface microlayer for geochemical and sedimentological purposes.

Erosion rates from these experiments are compared to other fine-sediment rate estimates in Fig. 8. The single points are values from three different sites at stresses of 1 dyne/cm². The broken lines are rates (Table 4) of four sites for stresses between 2 and 5 dynes/cm². These may be compared to the only previously available rate estimate from Puget Sound (line #1) and rates measured on San Francisco Bay Muds (lines #2 and 3) by Parthenaides (1965). The earlier estimate (line #1) falls below the new rate estimates at 1 dyne/cm² and above the rates at all sites measured in these experiments at 2 dynes/cm² (Fig. 8). This interposed position is somewhat encouraging considering the great dissimilarity in the two entrainment rate approaches.

The apparent differences in erosion rates at 1 dyne/cm² and at higher stress point out the need for more detailed study of entrainment rates in the 0-2 dyne/cm² stress range. This is particularly true for Puget Sound where at most deep sites naturally imposed bottom stress will generally not exceed more than 2 dynes/cm². At low stresses, however, the vertical distribution of resuspended material in the resuspension apparatus may not be uniform. If it is not, the concentration profiles must be measured. Thus, changes in the resuspension apparatus, making it more like that of Rouse (1938), would have to be made to acquire the necessary subsamples.

Information on the sizes of entrained particles comes from the Coulter Counter analysis (Fig. 9). For the two samples examined, at several stress levels, median diameters were 7.7-10.9 μm at Point Wells and 16.7-17.8 μm in Hood Canal. There is no significant change in median diameter or distributional shape for the Hood Canal samples over four stress levels. For the Point Wells samples, the median diameter and the distribution of size is moderately variable, with proportionately more large particles ($32 \mu < d < 80 \mu\text{m}$) at a stress of 1 dyne/cm² than at higher stress. The relative stability of

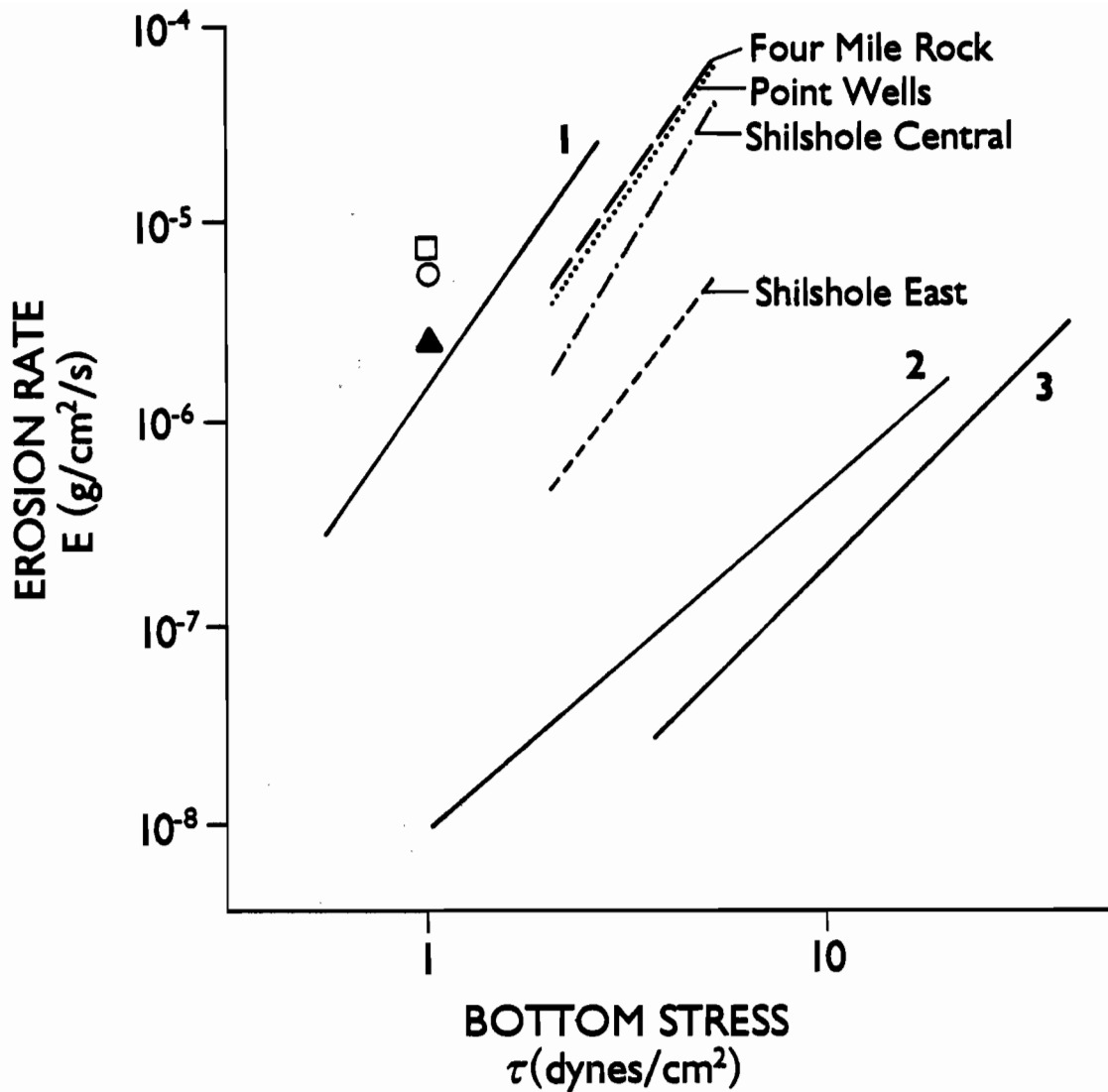


Figure 8.--Rates of erosion measured in these experiments compared to the rate of erosion calculated by Lavelle et al. (1984) at a location near the Shilshole-Central site (line 1), based on near-bottom current and transmissometer time series data. The single points are the erosion rates from these experiments at 1 dyne/cm² at Shilshole-Central (circle), Four Mile Rock (square), and South Hood Canal (triangle). Broken lines are erosion rates at 2 dynes/cm² and beyond measured in these experiments. Lines 2 and 3 are results on San Francisco bay muds (Parthenaides, 1965).

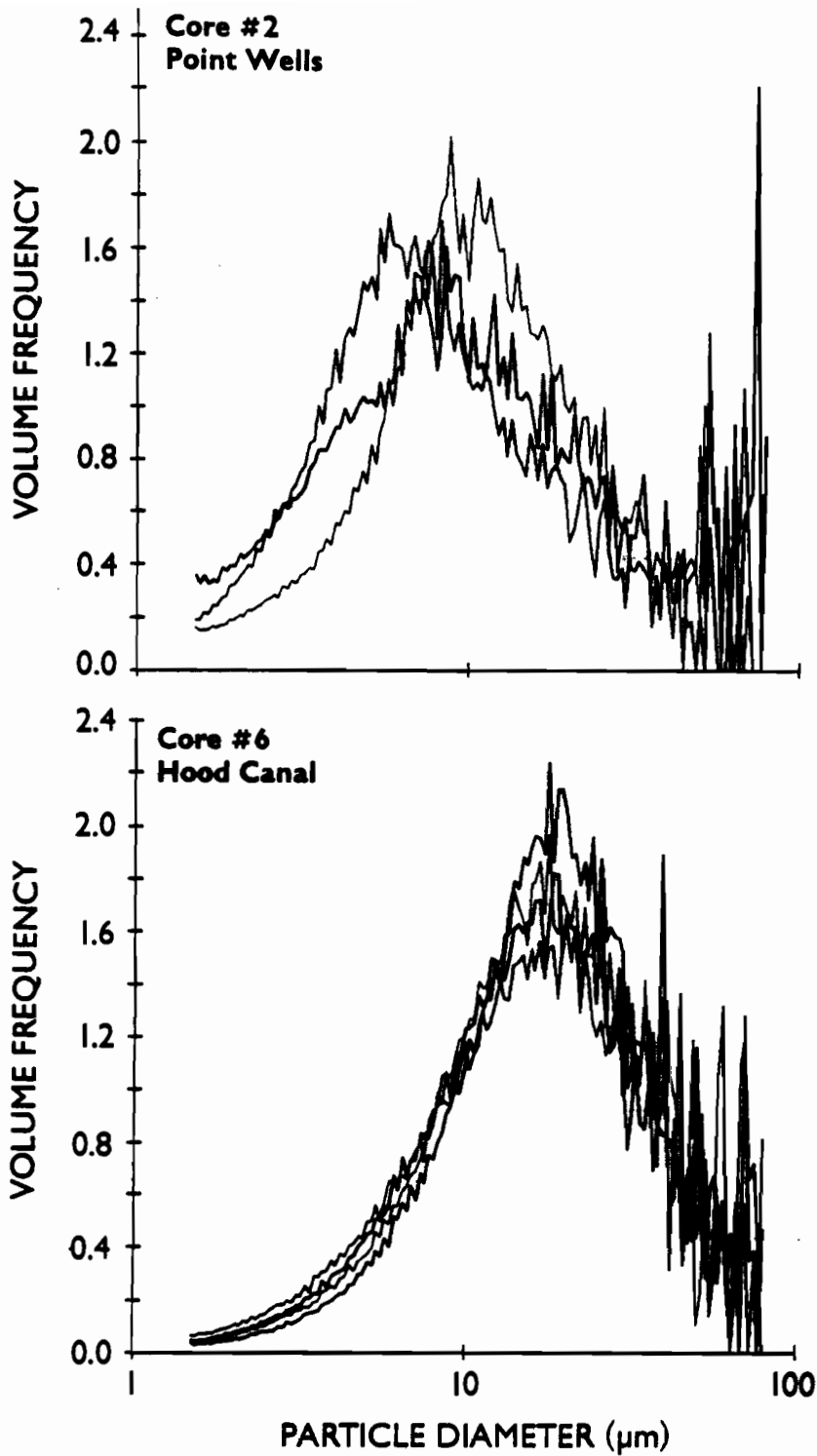


Figure 9.--Coulter Counter volume versus size distributions for the Hood Canal and Point Wells cores at various levels of equivalent bottom stress.

the size distributions through stress changes does suggest that the oscillating plate of the device does not progressively disaggregate particles at higher and higher stresses, if aggregates are in fact entrained.

Deposition velocities (Eq. 10) can be expected to have values comparable to particle settling velocities. Table 2 shows the range of calculated w_d range from 4.6×10^{-3} to 1.2×10^{-1} cm/s. Spherical quartz particles with diameters of 6-35 μm would have a similar range. The largest of the velocities inferred comes from the Shilshole-Central sample at a stress of 1 dyne/cm². Near that site, Lavelle et al. (1984) found in surficial samples a large range of particle sizes and concluded from time series measurements that a significant fraction of the resuspended material had a mean settling velocity of 1.0×10^{-1} cm/s. This value is much like the deposition velocity at low stress at the Shilshole-Central site (1.2×10^{-1} cm/s). Particles contributing to the surficial layer were thought to be fecal pellets and pellet fragments. Particles underlying the thin surficial layer are likely to be smaller in size. As these particles are increasingly entrained into the overlying fluid under increasing stress, the mean settling velocity of particles in suspension, and, consequently, the deposition velocity should decrease, as Table 2 in fact generally suggests. Note that for the Point Wells and Hood Canal samples, for which size distribution changes (Fig. 9) are small, there is very little change in deposition velocities at different stresses (Table 2).

5. CONCLUSIONS

Evidence from sites in the deeper parts of Puget Sound gathered with a device measuring entrainment potential of sediments suggest these tentative conclusions: 1) a thin (<1 mm) surficial layer of the sediment column is more

easily eroded than sediment below it; 2) entrainment rates at stresses of 2 dynes/cm² and above are not significantly different, at least for the four stations for which there were sufficient data to allow such a comparison. The thin layer first eroded is likely to be less consolidated sediment recently deposited on the sediment surface. This material, based on evidence from Coulter counting and deposition velocities, has a size distribution with median diameters ranging from approximately 7-18 μm. For sediment below the thin surficial layer the dependence of erosion rate on stress appears to be a power law with a power of two to three. Rates of erosion at 1 dyne/cm² are on the order of $2-7 \times 10^{-6}$ g/cm²/s.

Conclusions must be regarded as tentative because detailed measurements of the performance characteristics of the resuspension device have not been made. Needed are laboratory experiments that validate or replace the many assumptions made in the analysis of the data. For example, no radial dependence of concentrations is presumed, though visual observations of the eroding surface suggest that some radial advection near the sediment surface is occurring. Also, the assumption of uniform vertical distributions of concentration requires validation or replacement by a procedure for measuring the vertical profile of concentration. This is especially important for measurements at low stress levels (<1 dyne/cm²) that are typical of many estuarine sites, including some in the deep basin and embayments of Puget Sound. Turbulence profiles within the chamber at various oscillation frequencies would be useful, as would instantaneous near-bed stress distributions in both zero-mean and non-zero-mean shear devices used for comparison purposes. A grid of the kind used by Rouse (1938) rather than a perforated disk is also likely to produce a more uniform turbulence field better suited to sediment resuspension measurements at low turbulent intensity

levels. Further development of the device borrowing on ideas presented by Rouse (1938) and those of Thompson and Turner (1975) is thus suggested.

6. ACKNOWLEDGMENTS

We thank the officer and crew of the NOAA ship *Miller Freeman* for their assistance in taking box cores, Sharon Walker for graciously performing shipboard Coulter Counter analysis, and Hal Mofjeld, John Paul, and Ed Dettmann for their comments on the draft manuscript. The work was supported by NOAA/Environmental Research Laboratories and by EPA/Environmental Research Laboratory-Narragansett.

7. REFERENCES

- Baker, E.T., 1984. Patterns of suspended particle distribution and transport in a large fjord-like estuary. *J. Geophys. Res.*, 89, 6553-6566.
- Bouvard, M., and H. Dumas, 1967. Application de la méthode de fil chaud à la mesure de la turbulence dans l'eau, Première Partie. *Houille Blanche*, 22, 257-270.
- Chatterjee, S. and B. Price, 1977. Regression analysis by example. *J. Wiley*, New York.
- Cromwell, T., 1960. Pycnoclines created by mixing in an aquarium tank. *J. Mar. Res.*, 18, 73-82.
- Davis, W.R. and S. MacIntyre, in press. The role of benthic fauna in sediment resuspension. *Cont. Shelf Res.*
- E, Xq and E.J. Hopfinger, 1986. On mixing across an interface in stably stratified fluid. *J. Fluid Mech.*, 66, 227-244.
- Grass, A.J., 1983. The influence of boundary layer turbulence on the mechanics of sediment transport. Proceedings of Euromech: Mechanics of Sediment Transport, B.M. Sumer and A. Müller, Eds., A.A. Balkema, Rotterdam, The Netherlands, 3-17.
- Hopfinger, E.J. and J.A. Toly, 1976. Spatially decaying turbulence and its relations to mixing across density interfaces. *J. Fluid Mech.*, 78, 155-175.
- Kranck, K., and T. Milligan, 1979. The use of Coulter Counter in studies of particle size distributions in aquatic environments. Bedford Inst. Oceanogr. Rpt. Series, Dartmouth, Nova Scotia, 48 pp.
- Lavelle, J.W., H.O. Mofjeld, and E.T. Baker, 1984. An in-situ erosion rate for a fine-grained marine sediment. *J. Geophys. Res.*, 89, 6543-6552.

- Lavelle, J.W., G.J. Massoth, and E.A. Crecelius, 1986. Accumulation rate of recent sediments in Puget Sound, Washington. *Mar. Geol.*, 72, 59-70.
- Lavelle, J.W., and H.O. Mofjeld, 1987. Do critical stresses for incipient motion and erosion really exist? *J. Hyd. Eng.*, 113(3), 370-385.
- Long, R.R., 1978. Theory of turbulence in a homogeneous fluid induced by an oscillating grid. *Phys. Fluids*, 21, 1887-1888.
- McDougall, T.J., 1979. Measurements of turbulence in a zero-mean-shear mixed layer. *J. Fluid Mech.*, 94, 709-431.
- Murray, S.P., 1969. Simulation of horizontal turbulent diffusion of particles under waves. In: *Proceedings 11th Conference on Coastal Engineering*, ASCE, New York, 446-466.
- Nichols, F.H., 1975. Dynamics and energetics of three deposit-feeding benthic invertebrate populations in Puget Sound, Washington. *Ecol. Monogr.*, 45, 57-82.
- Parthenaides, E., 1965. Erosion and deposition of cohesive soils. *ASCE, J. Hydrol. Div.*, 91(HY1), 105-139.
- Parthenaides, E., 1972. Results of recent investigations on erosion and deposition of cohesive sediments. In: *Sedimentation*, H.W. Shen, ed., Fort Collins, CO, 20/1-20/38.
- Roberts, R.W., 1974. Marine sedimentological data of the internal water of Washington State (Strait of Juan de Fuca and Puget Sound). *Spec. Rep. 56*, Dept. of Oceanography, Univ. of Wash., Seattle.
- Rouse, H., 1938. Experiments of the mechanics of sediment suspension. *Proceedings, Fifth Congress for Applied Mechanics*, 55, J. Wiley, New York, 550-554.
- Rouse, H. and J. Dodu, 1955. Diffusion turbulente à travers une discontinuité de densité. *Houille Blanche*, 10, 522-529.

- Thompson, S.M. and J.S. Turner, 1975. Mixing across an interface due to turbulence generated by an oscillating grid. *J. Fluid Mech.*, 67, 349-368.
- Tsai, C.H. and W. Lick, 1986. A portable device for measuring sediment suspension. *J. Great Lakes Res.*, 12(4), 314-321.
- Turner, J.S. and E.B. Kraus, 1967. A one-dimensional model of the seasonal thermocline. I. A laboratory model and its interpretation. *Tellus*, 19, 88-97.
- Ward, P.R.B. and R. Chikwanha, 1980. Laboratory measurements of sediment by turbidity. *ASCE, J. Hyd. Div.*, 106(HY6), 1041-1053.
- Young, R.A., 1977. Seaflume: a device for *in-situ* studies of threshold erosion velocity and erosional behavior of undisturbed marine muds. *Mar. Geol.*, 23, M11-M18.